C. Riess et alii, Frattura ed Integrità Strutturale, 37 (2016) 52-59; DOI: 10.3221/IGF-ESIS37.08

Focussed on Multiaxial Fatigue and Fracture

The non-proportionality of local stress paths in engineering applications

C. Riess, M. Obermayr
ZF Friedrichshafen AG, DTGS1, 88038 Friedrichshafen, Germany
christian.riess@zf.com, http://orcid.org/0000-0002-8784-5297
martin.obermayr@zf.com, http://orcid.org/0000-0002-7672-8685

M. Vormwald
Technische Universität Darmstadt, Materials Mechanics Group, Franziska-Braun-Str. 3, D-64287 Darmstadt, Germany
vormwald@wm.tu-darmstadt.de, http://orcid.org/0000-0002-4277-785X

ABSTRACT. A scalar measure, which describes the non-proportionality of local stress paths in engineering applications, is introduced. For this purpose the moment of inertia approach by Meggiolaro is modified in a way that the stress time history is evaluated in a tresca-stress-space. This modification makes the non-proportionality factor invariant with respect to the coordinate system. An optimization procedure is implemented to derive a test set-up for new component tests with 2 load channels. The aim of the planned tests is to get a high non-proportionality at the potential crack initiation site. It is not possible to obtain a high non-proportionality factor at the failure location without selective weakening of the component (housing of a rear axle steering). Therefore specific areas of the structure are cut out and the optimization procedure is repeated. As a result of the optimization a test set-up with high local non-proportionality at the potential crack initiation site is achieved for the weakened structure. Another set-up with slightly less non-proportionality but with a very localized damage is derived. This set-up is preferred, because of the robustness in the physical test.

KEYWORDS. Non-proportional fatigue; Multiaxial testing.

INTRODUCTION

Many components in engineering applications are subjected to multiple and uncorrelated loads during service-life. Thus multiaxial stress states with rotating principal directions may occur. It is therefore useful to introduce a scalar measure (e.g. in the range of 0 to 1), which describes the non-proportionality of a local stress path. There are many approaches to characterize the non-proportionality in literature. One possibility is to directly consider the non-proportionality and the additional non-proportional hardening in an incremental plasticity model (see e.g. [1]). In this case, the non-proportionality is evaluated at every time step and transient effects may be taken into account. A second group of approaches determines the non-proportionality of a single cycle. An example for this group is the rotation factor according to Kanazawa [2]. A last group of non-proportionality factors (NPF) was developed to efficiently describe the non-proportionality of a whole stress time history [3-6].

NON-PROPORTIONALITY FACTOR FOR STRESS TIME HISTORIES

First ideas to describe the non-proportionality of local stress paths based on moments of inertia (MOI) stem back to Chu [7]. Bishop [3] seized this suggestion and introduced the first inertia based out-of-phase measure. The inertia based methods differ in the way the MOI is evaluated. Bishop calculates MOI with respect to the perimeter centroid (PC) of the path. For discrete data the evaluation is done using a weighted sum with the length of each segment as weighting factor.

Another inertia based method is proposed by Gaier [4]. In contrast to Bishop, Gaier calculates MOI with respect to the origin. Another difference is that Gaier doesn't use the length of a segment as weighting factor. Instead every stress state has the same mass. This formulation is only suitable for stress paths which are equally spaced in time. A small rainflow projection (RP) filter [8] may have large effects on the NPF.

Bolchoun [5] introduced a method without the use of MOI. The formulation is based on the correlation coefficient $Cor(f,g)$ of two functions f and g. The correlation coefficient of the time history of normal stress $\sigma'_x = \sigma'_x(t,\vartheta)$ and the time history of shear stress $\tau'_{xy} = \tau'_{xy}(t,\vartheta)$ is evaluated in all cutting planes ϑ. In order to make the NPF (f_{np}^B) invariant with respect to the coordinate system (CS), an average over all cutting planes is computed.

A disadvantage of the NPFs according to Bishop, Gaier und Bolchoun is, that they wrongly predict a high NPF for the stress path $\sigma_x = \sigma_y = \sin(t)$, $\tau_{xy} = \cos(t)$. Though, for this special case of equi-biaxial tension with out-of-phase torsion the directions of principal axes remain constant and therefore the planes of maximum shear stress do not change [6].

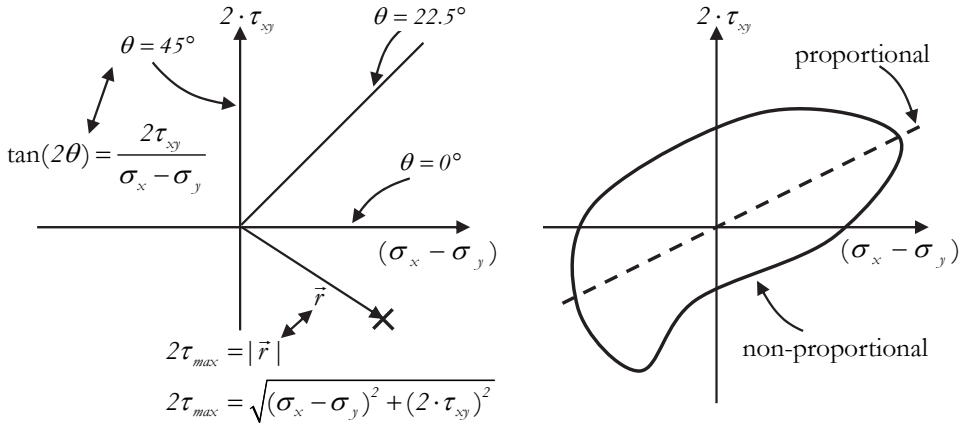

Figure 1: Interpretation of the tresca-diagramm (left) and non-proportional path (right).

That is why Meggiolaro [6] proposes to evaluate NPFs independent from hydrostatic stresses. According to Meggiolaro for plane state of stresses the evaluation of MOI should be based on a $\{(\sigma_x - \sigma_y) | \sqrt{3}\tau_{xy}\}$ stress-space. As a result of choosing this stress-space, the NPF is dependent on the choice of the CS. It is therefore suggested to use a tresca-stress-space $\{(\sigma_x - \sigma_y) | 2\tau_{xy}\}$ in order to make the NPF invariant with respect to the CS. In the tresca-diagram (see Fig. 1) every line through the origin is a line with constant principal axis (and constant angle of the maximum shear plane). Furthermore, the norm of a point in the diagram is equal to the double maximum shear stress $2\tau_{max}$.

Choosing the tresca-diagram, the calculation of the NPF is reduced to a geometrical 2D problem. The evaluation is performed according to the MOI method by Meggiolaro [9] on the basis of pseudo-elastic stress paths. By means of the tresca-diagram, MOIs I_{xx}^O, I_{yy}^O and I_{xy}^O are calculated with respect to the origin of the diagram as contour integrals along the stress path

$$I_{xx}^O = \frac{1}{L}\oint\left(2\tau_{xy}\right)^2 dp,\ I_{yy}^O = \frac{1}{L}\oint\left(\sigma_x - \sigma_y\right)^2 dp,\ I_{xy}^O = -\frac{1}{L}\oint 2\tau_{xy}\left(\sigma_x - \sigma_y\right) dp \tag{1}$$

where L is the total length of the stress path and dp denotes the length of an infinitesimal segment of the path. A detailed description for the evaluation of contour integrals of discrete 2D paths can be found in [8]. Principal moments of inertia λ_1^O and λ_2^O ($\lambda_1^O > \lambda_2^O$) are calculated by transformation into the principal coordinate system:

$$\lambda_{1,2}^O = \frac{I_{xx}^O + I_{yy}^O}{2} \pm \sqrt{\frac{\left(I_{xx}^O - I_{yy}^O\right)^2}{4} + \left(I_{xy}^O\right)^2} \tag{2}$$

Finally, the NPF is defined as root of the ratio of both principal MOI:

$$f_{np} = \sqrt{\lambda_2^O / \lambda_1^O} \tag{3}$$

Similar to the herein proposed method, the NPF may also be calculated using Bishop's method and the tresca-diagram. Then, the only difference is the evaluation of the MOIs with respect to the perimeter centroid and not with respect to the origin. This NPF is named f_{np}^{PC} and is only capable to describe the the out-of-phase extent of a stress path.

Examples in engineering applications

The non-proportionality at the crack initiation sites of several tests with 3 load channels and variable amplitude loadings is examined. Quite similar results are obtained using f_{np}^{PC} and f_{np}^{B}, because both NPFs only describe the out-of-phase extend of the stress path. In some cases there is an obvious difference to the results of f_{np}.

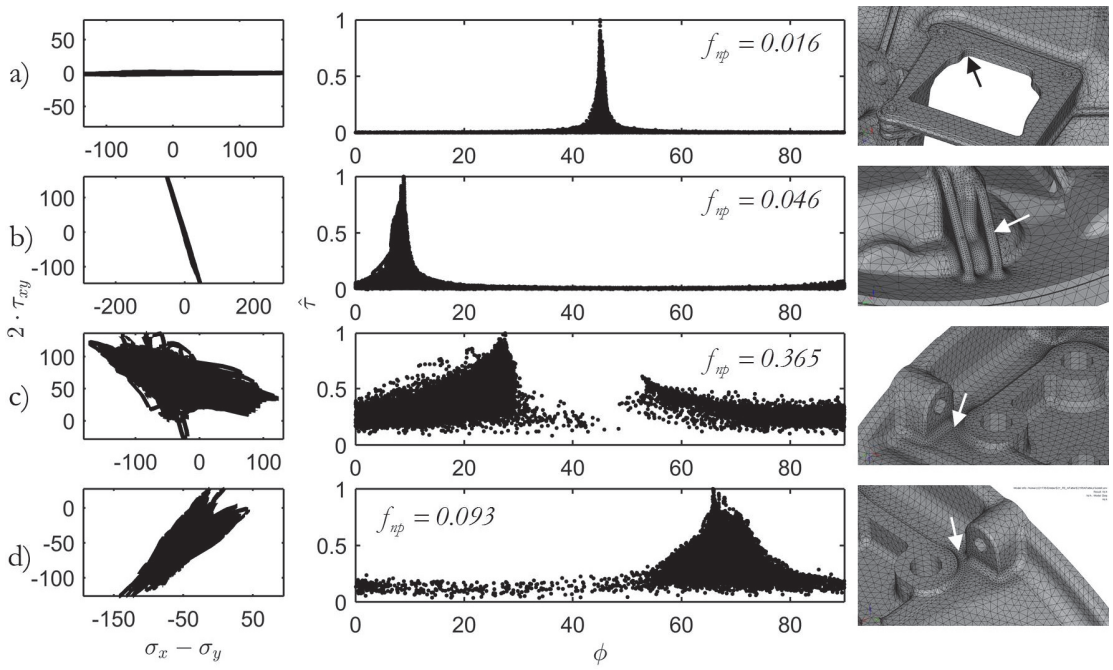

Figure 2: Tresca-diagram (left), changes of maximum shear planes (middle) and corresponding crack initiation site (right).

Four significant examples are extracted from the internal database and discussed in detail. The local stress paths at the crack initiation sites are displayed on the left of Fig. 2. The normalized maximum shear $\hat{\tau} = \tau_{max}(t) / \max(\tau_{max}(t))$ over the corresponding angle ϕ is plotted in the middle of this figure. Examples a and b indicate an almost uniaxial stress state with small changes in principal directions, which corresponds to small rotation of the planes of maximum shear. The NPFs at the crack initiation sites are 0.016 and 0.046, respectively. The crack initiation sites are located at a milled-out portion (a) and a die-cast rib (b). At examples c and d the crack initiation sites are located at a notch between two flanges. Both of them have almost the same out-of-phase extent ($f_{np}^{PC} = 0.3$). However, there are large differences in the NPF

f_{np}. The reason for the differences is identified in the nonzero mean values of the paths. Non-proportionality is increased ($f_{np} = 0.365$) in the case of example c because of the translation of the perimeter centroid. Whereas the translation of the PC in example d produces a lower rotation of maximum shear planes at high stress levels. The shape of the peak in the middle diagram is more distinct than in example c. Therefore, the non-proportionality is much lower ($f_{np} = 0.093$).

SYSTEMATIC PLANNING OF COMPONENT TESTS

In order to expand the experimental database, new component tests with 2 load channels and a high degree of local non-proportionality are planned. The housing of a rear axle steering is chosen for these tests (see Fig. 3). The component is mounted onto a steel plate. One of the forces F_1 shall be applied at the front drill hole and shall be aligned in the x-z-plane. The second force F_2 shall be applied at the upper drill hole and shall be aligned with the centerline of the drill hole. Finally, the angle φ (between x-axis and F_1) and the ratio of the forces $\lambda = F_1 / F_2$ remain as free variables for an optimization process.

For a given combination of φ and λ the pseudo-elastic stress path $\boldsymbol{\sigma}^*(\boldsymbol{x},t)$ for all nodes can be attained by calculation of three unit load cases (ULC) $\boldsymbol{\sigma}^*_{ULC}(\boldsymbol{x})$:

$$\boldsymbol{\sigma}^*(\boldsymbol{x},t) = \sin(t)\left[a_1 \cdot \boldsymbol{\sigma}^*_{ULC,1x}(\boldsymbol{x}) + a_2 \cdot \boldsymbol{\sigma}^*_{ULC,1z}(\boldsymbol{x})\right] + \cos(t)\left[a_3 \cdot \boldsymbol{\sigma}^*_{ULC,2}(\boldsymbol{x})\right]. \tag{4}$$

The relation between the scaling factors of the ULC a_1, a_2 and a_3 and the free variables φ and λ is as follows:

$$a_1 = \frac{1}{\sqrt{\left(1+\tan^2\varphi\right)\left(1+\frac{1}{\lambda^2}\right)}},\ a_2 = a_1 \cdot \tan\varphi,\ a_3 = a_1 \cdot \frac{\sqrt{1+\tan^2\varphi}}{\lambda}. \tag{5}$$

The challenge of the optimization is that the location with the highest damage $\boldsymbol{x}_{crit}$ is not known a priori. Depending on the choice of φ and λ the potential crack initiation site has to be determined numerically. Furthermore the change of $\boldsymbol{x}_{crit}$ results in a non-steady objective function $f_{np}(\boldsymbol{x}_{crit}) = f(\varphi,\lambda)$. That is why a genetic algorithm [10] is used to implement the optimization process.

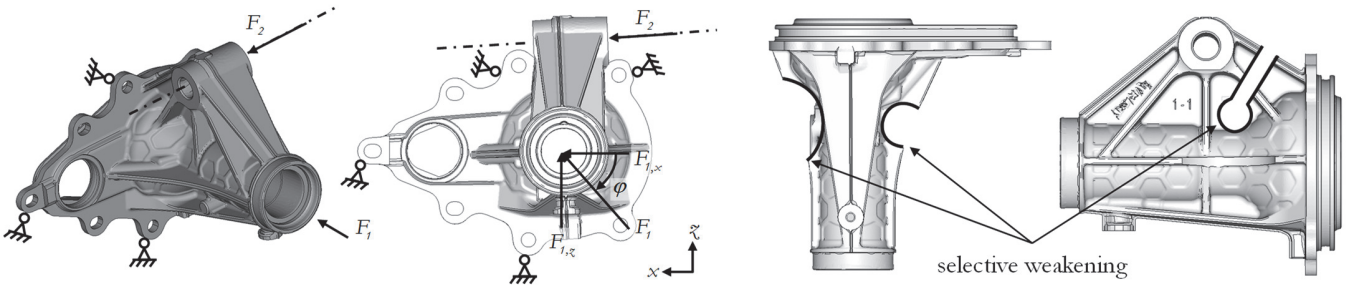

Figure 3: Housing of a rear axle steering subjected to two load channels (left) and selective weakening of the component (right).

Identification of the critical location x_{crit}

The fatigue assessment of non-proportional stress histories with rotating principal axis requires complex calculation algorithms, see [11, 12]. With regard to the optimization it is not necessary to perform a quantitatively precise damage calculation. It is rather important to qualitatively identify the critical location. Therefore, the identification of the critical locations is based on simple damage parameters and pseudo-elastic stresses.

Three different approaches for the identification of $\boldsymbol{x}_{crit}$ are discussed: the Findley parameter f [13], the normal stress amplitude in critical plane $\sigma_{a,cp}$ and the signed von Mises amplitude $\sigma_{a,v}$. The critical plane technique was especially invented for the case of rotating principal axis. One of the first damage parameters based on stresses in a specific plane of the material is the Findley parameter:

$$f = \max\left(\tau_{a,\vartheta} + k \cdot \sigma_{max,\vartheta}\right). \tag{6}$$

Besides the shear stress amplitude $\tau_{a,\vartheta}$ in the cutting plane with angle ϑ, this parameter also considers the maximum normal stress $\sigma_{max,\vartheta}$ in the same plane. The normal stress portion is weighted by an influence factor k, which can be determined for a given fatigue strength ratio σ_w / τ_w [14]. A given ratio of $\sigma_w / \tau_w = 1.5$ results in $k = 0.352$. The maximum of the parameter is searched numerically over a discrete number of cutting planes.
Another parameter, which is widely used in the industrial practice for brittle materials, is the normal stress amplitude in the critical plane $\sigma_{a,cp}$. Similar to the Findley parameter, a normal stress amplitude $\sigma_{a,\vartheta}$ has to be evaluated for all cutting planes and the maximum has to be searched numerically:

$$\sigma_{a,cp} = \max\left(\sigma_{a,\vartheta}\right). \tag{7}$$

As the third possibility for the identification of $\boldsymbol{x}_{crit}$ a signed von Mises approach is investigated. For this purpose, the time history of the Mises equivalent stress $\sigma_v(t)$ is assigned with the sign of the hydrostatic stress:

$$\sigma_v(t) = \operatorname{sign}\left(\sigma_{xx} + \sigma_{yy}\right) \cdot \sqrt{\sigma_{xx}^2 + \sigma_{yy}^2 - \sigma_{xx}\sigma_{yy} + 3\tau_{xy}^2}. \tag{8}$$

This approach results in discontinuities in the time history when applied to non-proportional stresses. A subsequent rainflow counting could identify unphysical cycles. Though, the unsteadiness has no effect in the case of constant amplitude loading and the equivalent amplitude is defined by the maximum $\sigma_{v,max} = \max\left(\sigma_v(t)\right)$ and the minimum $\sigma_{v,min} = \min\left(\sigma_v(t)\right)$ of the time history:

$$\sigma_{a,v} = \left(\sigma_{v,max} - \sigma_{v,min}\right) / 2 \tag{9}$$

There is no need for a numerical search over all cutting planes for this parameter, reducing the numerical expense.
The critical location $\boldsymbol{x}_{crit}$ is defined as the node, which has the highest value of the damage parameter according to Eqs 6, 7 or 9. Possible size effects (stress gradient, statistical, technological) are not considered.

Constraints

In order to prevent failure in an „unwanted“ region of the component, a node set $\boldsymbol{s}_{bc}$ may be defined. If the critical location $\boldsymbol{x}_{crit}$ (for a given parameter value φ_0 and λ_0) is part of the set $\boldsymbol{s}_{bc}$, the objective function $f_{np}\left(\boldsymbol{x}_{crit}(\varphi_0, \lambda_0)\right)$ is set to 0. Thus, it is not possible to get a solution with $\boldsymbol{x}_{crit}$ in an unwanted region. Examples are nodes, which are located at the gate system of the cast part, where the geometry is not well defined in reality. Therefore, these nodes are „unfavourable” and added to the set $\boldsymbol{s}_{bc}$.

Selective weakening of the component

It turns out, that it is not possible to obtain a high NPF at the failure site without selective weakening of the component. All critical nodes are located near the flange at the transition to the ribs. The stresses are highly oriented at these locations. Therefore specific areas of the structure are cut out (see Fig. 3) and the optimization procedure is repeated. As a result of

the weakening, the critical locations are shifted towards the middle of the component. Hence, effects due to the load introduction and the bolted connections are minimized.

RESULTS

Results of the optimization can be found in Tab. 1. Beside the solution parameters φ_{opt} / λ_{opt} the value of the objective function $f_{np,opt}$ is also listed. In the case without weakening of the structure, the results for the different versions are quite similar. Independent of the damage parameter, the same critical node is identified. It is not possible to attain a NPF higher than 0.16 at the potential crack initiation site.

	damage parameter	φ_{opt}	λ_{opt}	$f_{np,opt}$
original structure	f	3.113	1.516	0.160
	$\sigma_{a,\varphi}$	3.139	1.441	0.153
	$\sigma_{a,v}$	0.0	1.536	0.159
weakened structure	f	0.983	0.904	0.812
	$\sigma_{a,\varphi}$	0.882	0.688	0.831
	$\sigma_{a,v}$	0.946	0.776	0.819

Table 1: Results of the optimization.

The selective weakening results in the desired effect. High non-proportionalities ($f_{np} > 0.8$) are obtained for all versions. Similar critical nodes are identified using the signed von Mises approach and the $\sigma_{a,\varphi}$ approach. A slightly different solution is found by the Findley parameter approach. In this solution the critical node $\boldsymbol{x}_{crit}$ is located some nodes away in contrast to both other versions.

DISCUSSION

There is a high non-proportionality in many regions of the component. However, stresses are often small in these regions and failure will not occur there. On the other hand, the non-proportionality is negligible at many crack initiation sites. Independent of the external loads the stresses are highly oriented at the crack initiation site in those cases. Typical examples are ribs of housings made by die-cast or a cross-hole in a shaft. These are locations, where the local stress states are nearly proportional.

In order to get a high non-proportionality the following two conditions have to be fulfilled: The unit load cases have to create stress states with different planes of maximum shear (different principal axis) and the forces have to be in an appropriate ratio. A systematic planning of component tests with high non-proportionality is only feasible using an automated optimization process.

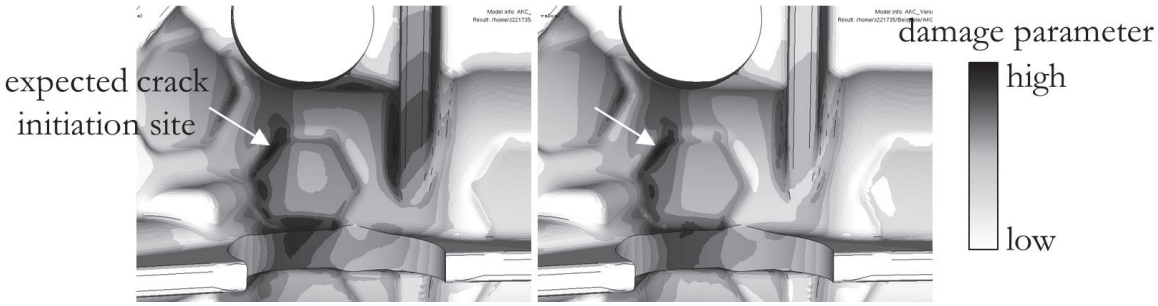

Figure 4: $\sigma_{a,v}$ for the result of the optimization (left) and the tradeoff (right).

An essential point of the optimization is the identification of critical locations. The aim of the identification is to find the node, which has the highest probability of crack initiation, in a simple manner. Size effects may have a large influence for notched components, but under non-proportional stresses they are not yet well defined. Thus, in this work notch support because of size effects is omitted. An explicit consideration of size effects could help to increase the accuracy of the identification. Therefore, the influence of size effects under transient stress gradients and transient highly stressed volumes or surfaces needs to be investigated.

To ensure, that the crack initiation site in the physical test coincides with the critical node $\boldsymbol{x}_{crit}$, a solution with a strong damage localization is favorable. The iterations of the optimization are scanned manually for solutions with higher localization of the damage parameter (see Fig. 4), but sufficiently high non-proportionality. A satisfactory parameter set (tradeoff) is identified ($\varphi = 0.9032$ and $\lambda = 1.2274$) with NPF of 0.572 at the critical node.

CONCLUSION

A new inertia based non-proportionality factor for the evaluation of pseudo-elastic stress paths is introduced. Calculations of the NPF are performed according to a modified version of the MOI method from Meggiolaro. The use of the tresca-diagram $\{(\sigma_x - \sigma_y) | 2\tau_{xy}\}$ makes the NPF invariant with respect to the coordinate system. Furthermore a numerical optimization, which searches for a test set-up with high non-proportionality at the potential crack initiation site, is developed and implemented. A selective weakening of the chosen component is necessary in order to get a high NPF at the critical location. A possible weak point of the optimization is that size effects are not considered. Therefore, further investigations should focus on the influence of size effects under non-proportional stresses. In order to get a robust test set-up, a tradeoff is derived. Experimental investigations with constant and variable amplitudes are going to be performed on the basis of this tradeoff.

REFERENCES

[1] Tanaka, E., A nonproportionality parameter and a cyclic viscoplastic constitutive model taking into account amplitude dependences and memory effects of isotropic hardening, Eur. J. Mech. A/Solids, 13 (1994) 155-173.

[2] Kanazawa, K., Miller, K.J. and Brown, M.W., Cyclic deformation of 1% Cr-Mo-V steel under out-of-phase loads, Fatigue Fract. Eng. Mater. Struct., 2 (1979) 217–228. DOI: 10.1111/j.1460-2695.1979.tb01357.x

[3] Bishop, J.E., Characterizing the non-proportional and out-of-phase extent of tensor paths, Fatigue Fract. Eng. Mater. Struct., 23 (2000) 1019-1032. DOI: 10.1046/j.1460-2695.2000.00355.x

[4] Gaier, C., Lukacs, A. and Hofwimmer, A., Investigations on a statistical measure of the non-proportionality of stresses, Int. J. Fatigue, 26 (2004) 331-337. DOI: 10.1016/j.ijfatigue.2003.08.023

[5] Bolchoun, A., Wiebesiek, J., Kaufmann, H., Sonsino, C.M., Application of stress-based multiaxial fatigue criteria for laserbeam-welded thin aluminium joints under proportional and non-proportional variable amplitude loadings, Theor. Appl. Fract. Mech., 73 (2014) 9-16. DOI: 10.1016/j.tafmec.2014.05.009

[6] Meggiolaro, M.A., Castro, J.T.P., Prediction of non-proportionality factors of multiaxial histories using the Moment Of Inertia method, Int. J. Fatigue, 61 (2014) 151-159. DOI: 10.1016/j.ijfatigue.2013.11.016

[7] Chu, C.C., Conle, F.A. and Hübner, A., An integrated uniaxial and multiaxial fatigue life prediction method, VDI Berichte, 1283 (1996) 337-348.

[8] Dreßler, K., Carmine, R., Krüger, W., The multiaxial rainflow method, in: Rie, K.T. (Ed.), Low cycle fatigue and elasto-plastic behaviour of materials, Elsevier Science Publ., London, (1992) 325-331.

[9] Meggiolaro, M.A., Castro, J.T.P., An improved multiaxial rainflow algorithm for non-proportional stress or strain histories – Part I: Enclosing surface methods, Int. J. Fatigue, 42 (2012) 217-226. DOI: 10.1016/j.ijfatigue.2011.10.014

[10] Xavier Blasco Ferragud, F., Control predictivo basado en modelos mediante tecnicas de optimizacion heuristica. Aplicacion a procesos no lineales y multivariables (PhD Thesis in Spanish), Universitat Politècnica de València, Spain, (1999).
[11] Hertel, O. and Vormwald, M., Multiaxial fatigue assessment based on a short crack growth concept, Theor. Appl. Fract. Mech., 73 (2014) 17-26.
DOI: 10.1016/j.tafmec.2014.06.010
[12] Hertel, O. and Vormwald, M., Short-crack-growth-based fatigue assessment of notched components under multiaxial variable amplitude loading, Eng. Frac. Mech., 78 (2011) 1614-1627.
DOI: 10.1016/j.engfracmech.2011.01.016
[13] Findley, W.N., A theory for the Effect of Mean Stress on Fatigue of Metals Under Combined Torsion and Axial Load or Bending, J. Eng. Ind., 81 (1959) 301-306.
[14] Socie, D.F. and Marquis, G.B., Multiaxial Fatigue, SAE, Warrendale, (2000).